Bonding and vibrational dynamics of a large π-conjugated molecule on a metal surface

2008 J. Phys.: Condens. Matter 20 224010

(http://iopscience.iop.org/0953-8984/20/22/224010)

J. Phys.: Condens. Matter **20** (2008) 224010 (10pp) doi:10.1088/0953-8984/20/22/224010

Bonding and vibrational dynamics of a large π-conjugated molecule on a metal surface

R Temirov[1,2], S Soubatch[1,2], A Lassise[1,2] and F S Tautz[1,2]

[1] Jacobs University Bremen, School of Engineering and Science, PO Box 750561 28725 Bremen, Germany
[2] Institut für Bio- und Nanosysteme 3, JARA, Forschungszentrum Jülich, 52425 Jülich, Germany

Received 8 November 2007
Published 13 May 2008
Online at stacks.iop.org/JPhysCM/20/224010

Abstract
The interplay between the substrate bonding of a large π-conjugated semiconductor molecule and the dynamical properties of the metal–organic interface is studied, employing the prototypical PTCDA/Ag(111) monolayer as an example. Both the coupling of molecular vibrations to the electron–hole-pair continuum of the metal surface and the inelastic scattering of tunnelling electrons by the molecular vibrations on their passage through the molecule are considered. The results of both types of experiment are consistent with the findings of measurements which probe the geometric and electronic structure of the adsorbate–substrate complex directly; generally speaking, they can be understood in the framework of standard theories for the electron–vibron coupling. While the experiments reported here in fact provide additional qualitative insights into the substrate bonding of our π-conjugated model molecule, their detailed quantitative understanding would require a full calculation of the dynamical interface properties, which is currently not available.

1. Introduction

Organic molecular semiconductors have been developed to a point where a range of devices, including light emitting diodes [1, 2], transistors [3, 4] and solar cells [5] with properties good enough for certain applications can be made. Interfaces are important functional elements in these devices [6], and hence a technological need to study interfaces between condensed molecular phases of large π-conjugated semiconductor molecules and inorganic solids arises, in addition to the fundamental interest in these interfaces.

The bonding of these molecules to metallic substrates is an important issue, because it affects the injection properties at the electrode contacts of organic devices. In contrast to the situation for small molecules, much less is known about the adsorption properties of large π-conjugated organic molecules. Conceptually, if a molecule adsorbs at a solid surface, this can occur either by chemical or by physical bonding. Chemical adsorption, or chemisorption, thereby refers to bonds of chemical strength (binding energies per adsorbate in the electron-volt range), whereas physical adsorption, or physisorption, refers to unspecific adsorption based on the dispersion interaction.

It has turned out that aromatic molecules, if they adsorb with their π-system parallel to the surface, may interact chemically with the metal surface [7, 8, 10]. Obviously, if an adsorbate is bonded chemically, the substrate will have a profound influence on the electronic properties of the molecule. Their modification can be detected with many experimental methods, e.g. photoelectron spectroscopy (UPS), scanning tunnelling microscopy and spectroscopy (STM/STS), x-ray adsorption spectroscopy (NEXAFS), and photoluminescence spectroscopy (PL).

In the present article we discuss the manifestations of the chemisorption interaction in the electron–vibron coupling at metal surfaces. It has long been recognized that at metal surfaces the coupling between electronic and nuclear degrees of freedom may influence many of the surface properties, such as surface reconstruction, surface phonon and electron dispersions, vibrational lifetimes and line shapes etc (see [10] for a recent review). Here we employ the coupling between the two types of excitations to gain additional insight into the molecule–substrate bonding; to this end, the dynamical properties of the chemically bonded adsorbate are studied and analysed in the light of their implications for the electronic

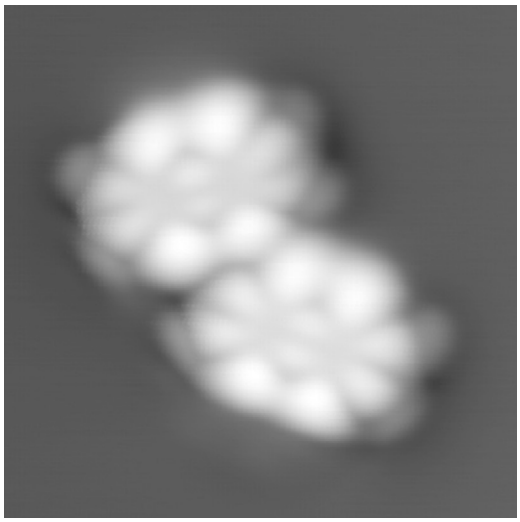

Figure 1. Submolecular STM contrast of two PTCDA molecules adsorbed on the Ag(111) surface. Scanning parameters: $U_b = -0.56$ V, $I = 0.6$ nA; image area 33×33 Å^2.

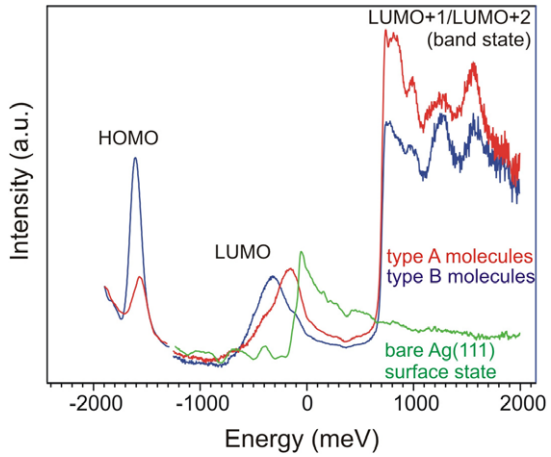

Figure 2. STS spectra of PTCDA on Ag(111), recorded as $\mathrm{d}I/\mathrm{d}V$ spectra using the lock-in technique. Red solid line: molecule of type A, aligned with the $[10\bar{1}]$ direction of Ag(111). Blue solid line: molecule of type B, misaligned by 17° with respect to the $[10\bar{1}]$ direction. Green solid line: surface state of clean Ag(111). In the range from −1250 to 2000 meV (−2000 meV to −1300) spectra on the molecule are recorded with a clean tip (functionalized tip) [21].

structure. In particular, we consider two experiments. First, we study the dipole activities and line shapes of molecular vibrations in electron energy loss spectroscopy (EELS). This yields insights into the coupling of the vibrations to the electron–hole-pair continuum that will contain signatures of the molecule–substrate bonding [11]. Second, we analyse the resonant tunnelling of the electrons through the molecular adsorbate layer and search for signs of the electron–vibron interaction in the tunnelling current. This technique is known as inelastic tunnelling spectroscopy (IETS). It can be used to study vibrational dynamics and electron–vibron coupling at the level of a single molecule [12].

We use the PTCDA/Ag(111) interface as our model system, because this interface is arguably among the best understood of any interfaces between large π-conjugated molecules and metals [6, 10, 11, 13–20]. But, before turning to the two experiments mentioned above, we first briefly review what is known about the molecule–substrate bond from experiments which probe the geometric and electronic structure of the adsorbate–substrate complex directly.

2. Bonding mechanism of PTCDA on Ag(111)

Let us begin our discussion of PTCDA bonding with an image of the molecule as it appears in scanning tunnelling microscopy on the Ag(111) surface (figure 1). The extreme resolution of this image is only achieved if a functionalized tip is employed [21]. A clean metal tip produces the same kind of pattern, but because of the lower resolution the two outer lobes at the long edges of the molecules merge into one, and the inner lobes are barely distinguishable [8, 19]. The STM imaging process of PTCDA on Ag(111) has been studied in detail in [8, 21]. But, irrespective of the tip state, the images which are observed from PTCDA for small positive and negative biases clearly resemble the charge distribution in the lowest unoccupied molecular orbital (LUMO) of the free PTCDA molecule, as a simple quantum chemical calculation shows [22].

The extremely high resolution of the images has enabled us to determine the actual adsorption site of the molecule [21]. The existence of a definite adsorption site cannot be taken for granted, because one may rightly ask what should make a large molecule which averages over many periods of the substrate corrugation potential adsorb site-specifically, especially if the molecule–substrate interaction is, as we will see below, to a large extent connected to the extended π-electron system of the molecule. On Au surfaces, for example, PTCDA and many other molecules form incommensurate overlayers, which even overgrow the herringbone reconstruction of the Au(111) surface without being influenced by the complex substrate structure [23, 24]. But on Ag(111), the molecule–substrate interaction is stronger than on Au(111) and a definite adsorption site ensues. It turns out that the two PTCDA molecules (type A and type B) contained in the unit cell of the monolayer herringbone pattern both adsorb in bridge sites [21]. Their different contrasts in the image (cf [21]) are therefore not related to distinct sites, but to unlike in-plane orientations of the molecules relative to the high-symmetry directions of the substrate and possibly to different intermolecular interactions [8, 21]. The bridge site is also predicted by density functional calculations [8], although the calculated binding energies are too large, because of general problems with density functional theory (DFT) on weakly interacting systems [8, 21]. Experimentally, the adsorption energy per molecule is not known, because the molecule does not desorb intact from the surface [25, 26], such that results from thermal desorption spectroscopy are not available.

Coming back to figure 1, it is remarkable that an originally empty orbital is imaged at negative bias voltages. This can only result from a substantial charge transfer into the molecule. The STS spectrum of figure 2 is dominated by three features and indeed confirms this charge transfer, in the sense that a state

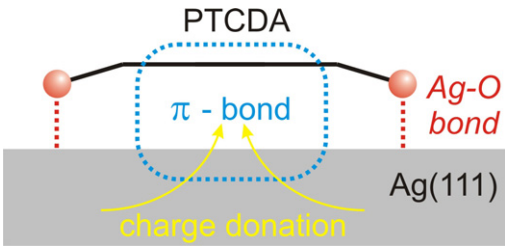

Figure 3. Schematic representation of the bonding interaction of PTCDA with Ag(111). Further discussion in the main text.
(This figure is in colour only in the electronic version)

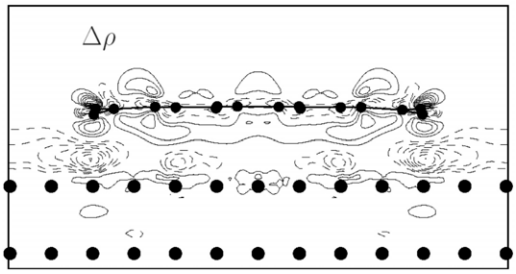

Figure 4. *Ab initio* calculation of the change in the electron density at the PTCDA/Ag(111) interface (side view). The quantity displayed is the difference between the self-consistent LDA charge density of the adsorption system minus the charge densities of the individual components (PTCDA molecule, Ag(111) surface) alone. For visualization, charge density difference has been integrated along the axis perpendicular to the drawing plane. Solid (dashed) lines correspond to positive (negative) electronic charge transfer. Details can be found in [8].

appears just below the Fermi level at −0.3 eV binding energy. Judging from its appearance in STM and STS images, this state must be the former LUMO (lowest unoccupied molecular orbital) of the molecule. We also note that this state is much broader than the peak at −1.7 eV, which by spectroscopic imaging is revealed as the former HOMO (highest occupied molecular orbital) [21]. The origin of the spectroscopic feature appearing at 1.0 eV has been discussed elsewhere [19].

Both the charge transfer into the LUMO and its broadening are indicative of chemical bonding. Since for any chemical bond the bond length is a valid parameter to characterize the bond strength, we have measured the vertical distance of PTCDA above the Ag(111) surface by the NIXSW technique [15, 16]. Additionally, the technique is suited for measuring the internal distortion of the adsorbed molecule. The following is found. First, the bonding distance of PTCDA to Ag(111) is substantially shorter (2.86 Å) than the interlayer distance in bulk PTCDA crystals (3.22 Å). The latter is commonly interpreted as a van der Waals bonding distance. Second, the molecule is distorted, with the carboxylic oxygen atoms 0.18 Å closer to the silver than the average carbon. It thus seems as if both the π-electron system and the carboxylic oxygen atoms are involved in the bonding to the substrate.

To see whether these two observations really support the scenario of a chemical interaction, we have repeated the NIXSW experiment on Au(111) [27], where all spectroscopic data reveal an essentially physisorptive bonding [7, 22, 28]. Indeed, properly accounting for the reconstruction and relaxation of the Au(111) surface, we find a much larger bonding distance of 3.27 Å [27], close to the van der Waals contact distance between carbon and gold. We note in passing that the larger contact distance on Au(111) and the electronic structure of the molecule on this surface agree well with each other, because it is found by STS on PTCDA on Au(111) that LUMO remains unoccupied upon adsorption [28, 29].

In the light of the PTCDA/Au(111) contact distance, the PTCDA/Ag(111) contact thus really looks like a chemisorptive one. To analyse the bonding more closely, the results of density functional calculations, of which several are available in the literature [8, 15, 16, 30–33], are most welcome. Unfortunately, their results are in disagreement with each other and partly also with experiment [8]. Some calculations do not reproduce the charge transfer which experiments unambiguously prove, while others do not find the molecular distortion. The calculated results depend strongly on the employed density functional. In state-of-the-art generalized gradient approximations, the bonding distance comes out far too large (3.22–3.40 Å) [15], while LDA gives a distance which is slightly too short [8]. Nevertheless, LDA still yields the best overall agreement with experiments [8, 21]. Other features of the interface which can be rationalized on the basis of DFT are the site-specific electronic structure and the distortion of the molecule [8, 21]. Moreover, STM images have been shown to be reliably reproduced by a Tersoff–Haman approach based on DFT-LDA calculations [8, 21].

On the basis of experiment and calculations, we can draw up the following picture of the PTCDA/Ag(111) interaction (figure 3). The molecule interacts with the Ag surface via its two functionalities. (1) The π-system hybridizes with states from the Ag 5s band and accepts charge from the metal. This is an extended interaction. (2) The carboxylic oxygen atoms form local bonds which certainly contain an electrostatic but possibly also a weak covalent component. At first sight it may seem as if these two interaction channels are independent of each other. However, if the influence of both interactions on the carbon skeleton is analysed, one finds them to be synergetic, in the sense that they contract and expand the same C–C bonds throughout the molecule [8].

Concerning the extended interaction, two questions arise. First, is this interaction a bonding one? One could argue that the larger distance of the central part of the molecule results from a repulsive interaction. However, since the behaviour of the former LUMO resembles the (bonding) Newns Anderson scheme quite closely (cf [6]) and since the DFT-LDA calculation finds a build up of charge between the molecule and the silver surface (figure 4 [8]), the interaction seems to be bonding rather than anti-bonding. In a simple model of an anti-bonding interaction, one would expect a wavefunction (and thus charge density) node between the two partners. This is definitely not observed in the calculation, which—in spite of its problems—models the experimentally observed spectroscopic signature of the interface quite well. But it is nevertheless true that distinct optimum distances in both bonding channels require a compromise with respect to the vertical distances, with the result that the distance of the central molecule may well be shorter than its optimum, while

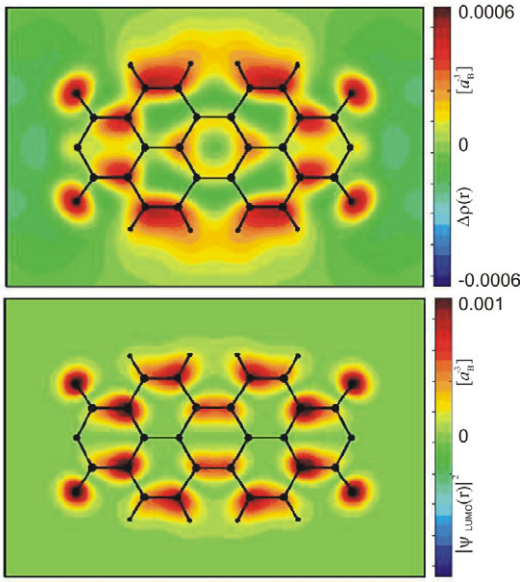

Figure 5. Top panel: horizontal cut through the PTCDA/Ag(111) interface for the type A molecule. The colour scale codes the change in local charge density $\Delta\rho(r) =$ (PTCDA + Ag)–PTCDA–Ag. Blue corresponds to an electron deficiency with respect to the superposition of the free Ag and free PTCDA, while red corresponds to an electron accumulation. Bottom panel: cut through the LUMO charge density of free PTCDA at a height corresponding to the cut in the top panel. The data is based on the calculation discussed in detail in [8].

the opposite is true of the corner oxygen atoms. In this sense, the oxygen atoms may actually pull the carbon skeleton into the repulsive part of the interaction potential.

The second question regarding the extended interaction is whether it can be responsible for a site-specific interaction. In principle, the answer is yes, because the LUMO consists of lobes of lateral sizes which are comparable to the characteristic length scale of the atomic corrugation potential of the substrate. Indeed, in figure 5 [8] we see that the accumulated charge between molecule and metal (the 'bond') does not have the same lateral distribution as the LUMO but exhibits contributions from the LUMO and the silver surface [8]. There is no reason why such a structured bond should not be site-specific. We can thus conclude that it is not necessarily the local oxygen bonds alone which are responsible for site specificity.

Finally, we stress the twofold role of the oxygen atoms for the substrate interaction. On the one hand, direct bonds with the substrate are formed. On the other hand, the electronegative anhydride groups increase the electron affinity of the π-electron system towards metal electrons, as the comparison with the perylene molecule shows: perylene interacts much more weakly with Ag(111) and at room temperature forms an orientationally disordered layer [34].

3. Coupling of molecular vibrations to electron–hole pairs

In a detailed theoretical study for CO on Cu(100), it has been shown that vibrational energy relaxation via EHP (electron–hole pairs) may be highly mode-selective [35–37]. The reason for the mode selectivity can be found in the chemical bond between adsorbate and substrate [38]. On the other hand, for weakly substrate-interacting adsorbates (adsorbate–substrate distances larger than approximately 3 Å), the dynamical coupling originates from electrostatic interactions and is therefore less mode-specific [39, 40]. In particular, chemical bonding may lead to the well-known mode-specific effect of interfacial dynamical charge transfer (IDCT), in which the coupling of EHP to adsorbate vibrations not only leads to increased line widths and line shifts, but also to the activation of certain vibrational modes which would otherwise be (nearly) suppressed by selection rules [38, 41, 42]. EHP coupling can therefore also change the observed intensities of selected spectral features. IDCT was first proposed by Persson and Persson for the stretching vibration of CO on Cu(100) [43] and also applied to, for example, the O–O stretching vibration of O_2 on Pt(111) [44] and C–H stretch vibrations of methoxide on Cu(100) [45]. For low-frequency vibrations of CO on Cu surfaces (hindered rotations), a similar phenomenon, namely the coupling of adsorbate vibrations to conduction electron currents, has been observed [46–49].

Recently, IDCT has also been reported both for C_{60} [50–53] and PTCDA [11, 54] on Ag(111) surfaces. Its mechanism is depicted schematically in figure 6. As can be seen in this figure, IDCT has two pre-requisites. On the one hand, one of the substrate-coupled adsorbate electronic levels has to be metallic, i.e. partially occupied. Such a level is shown schematically in figure 6(a). Second, there needs to be an appreciable electron–vibron coupling in the combined molecule–substrate complex such that, on excitation of certain vibrational modes, the energetic position of the metallic hybrid orbital is modulated. This will lead to the excitation of EHP and dynamical charge transfer across the metal–adsorbate interface, as is also indicated in figure 6(a). By this mechanism, totally symmetric modes of the adsorbate, which are otherwise suppressed by the dipole selection rule in any spectroscopy which relies on dynamical dipole moments (infrared spectroscopy, electron energy loss spectroscopy, but not Raman spectroscopy), can be activated by the perpendicular charge transfer across the interface, as shown in figure 6(c) for mode 2.

The above-mentioned mode selectivity of EHP/molecular vibration coupling in the presence of chemical interaction, if indeed observed in experiment, can be used to learn more about detailed features of the chemical adsorbate–substrate bond, because the vibrational modes act as in-built probes regarding the adsorbate–substrate coupling. If a mode is particularly strongly enhanced and/or shows a characteristic (i.e. broad or asymmetric) line profile (mode 2 in figure 6), the corresponding dynamic distortions must couple very effectively to EHP. The ansatz to probe the chemical interaction by studying the selectivity of chemical EHP coupling is particularly promising for large molecules, such as, for example, PTCDA, which have many internal mechanical degrees of freedom, some of them localized to certain parts of the molecules or even single bonds. Such modes are excellent 'spies' of the local chemical interaction

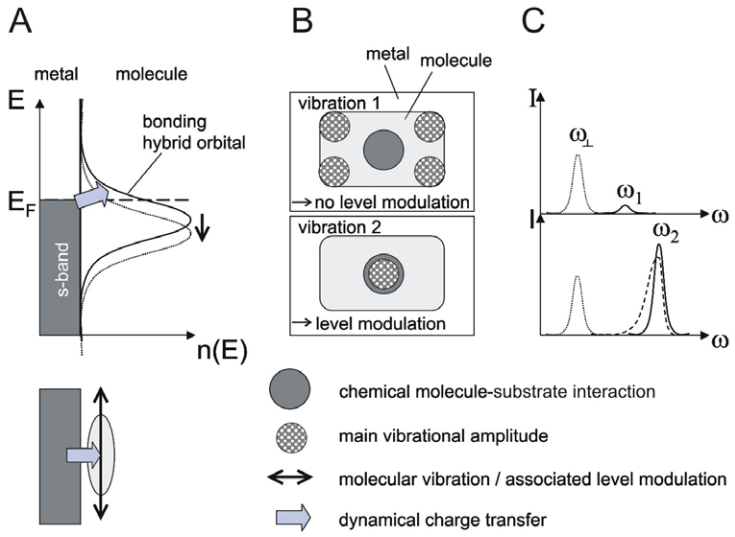

Figure 6. Schematic representation of the mechanism of interfacial dynamical charge transfer (IDCT). (a) A partially occupied bonding hybrid orbital is modulated by the excitation of a molecular vibration. This leads to the excitation of EHP, and charge oscillates between metal and molecule, as shown in the side view of the adsorbate. (b), (c) Schematic illustration of a model that rationalizes which parallel-polarized (i.e. in-plane) vibrational modes will be activated by IDCT. (b) Top view of an adsorbed molecule. The location of the chemical molecule–substrate bond is indicated by dark grey circles. Hatched circles indicate which parts of the molecule are primarily affected by each of the two molecular vibrations. (c) Vibrational spectra corresponding to the two situations sketched in (b). Vibration 1 will remain weak, while vibration 2 will be strongly enhanced. For reference, the amplitude of a typical vibration with perpendicular (i.e. out-of-plane) polarization is also given.

between adsorbate and substrate, as illustrated schematically in figures 6(b) and (c). Indeed, selectivity of EHP coupling has been observed for our model molecule PTCDA, and it has been used for characterizing its chemical bond to Ag(111) [13, 22]. The main aspects of the argument are summarized below. Incidentally, the results to be presented in this context are in full agreement with the spectroscopic and structural investigations discussed in section 2.

IDCT needs metallicity (partial occupancy) of an electronic level of the adsorbate [11, 43]. As we saw above, such partial occupancy is in the present case provided by chemisorption, which stabilizes the partially filled affinity level of the molecule slightly below the Fermi level. Very strong additional evidence for partial occupancy comes from the observation of energy loss spectra of PTCDA monolayers on Ag(111), which show a strong loss continuum, starting at zero loss energy, peaking at approximately 400 meV and extending beyond 1 eV [11, 17] (figures 7(c) and (d)). This continuum can be assigned to EHP excitations involving metal–molecule hybrid levels close to the Fermi energy (figure 2). Incidentally, no metallicity was observed for any of the other noble metal substrates which have been studied (Au(111), Ag(100), Ag(110), and Cu(111)) [22, 29].

Turning to the vibrational spectra of PTCDA/Ag(111) monolayers in figure 7 (spectrum 7(d)), one first sees a very strong enhancement of parallel-polarized modes above 900 cm^{-1}. A detailed analysis shows that these modes are totally symmetric, Raman active modes of the molecule. The mechanism by which these modes are activated is the interfacial dynamical charge transfer explained above [11]. Some of the activated modes (labelled A and B in figure 7) in fact exhibit an asymmetric line shape. This is due to a mechanism first suggested by Fano [55] and applied to EHP coupling by Langreth *et al* [56, 57], in which a continuum of states (here EHP) is coupled non-adiabatically to discrete levels (here certain molecular vibrations of PTCDA). The Fano line shape, in the form introduced by Rice *et al* [58–60], has actually been used to fit the spectrum in figure 7(d) (cf [11]) and to calculate an electron–phonon coupling constant of the system [11], in good agreement with other data [61].

Coming back to the issue of selectivity, it was noted in [13, 22] that, out of the 17 totally symmetric modes of PTCDA, four modes are enhanced by IDCT particularly strongly (indicated by arrows in figure 7). According to figure 6, this must mean that for these modes the modulation of the partially occupied electronic level is particularly large. Following the idea of using the selectively enhanced modes as probes of the local chemical interaction, we have in [13, 22] performed density functional calculations of vibrationally excited free molecules, with the aim of identifying those locations in the molecule where the four modes in question produce internal charge density modulations to which the metal electrons are likely to respond strongly with a compensating charge flow perpendicular to the surface (which leads to the selective activation of these four modes). Since, on the other hand, such dynamical charge flow will preferentially occur in regions where the metal–molecule coupling is strong, this is a way of probing the latter in real space, as indicated schematically in figure 6(b). This idea can also be formulated in terms of the energy diagram in figure 6(a): the modulation of the energy position of the bonding level, which is necessary for the selective enhancement of a certain mode, can only be effected by vibrations which distort the local charge distribution in the chemisorption bond. As a result of this analysis in [13, 22], it has turned out that the centre of the molecule plays an important role in the bonding. It has been

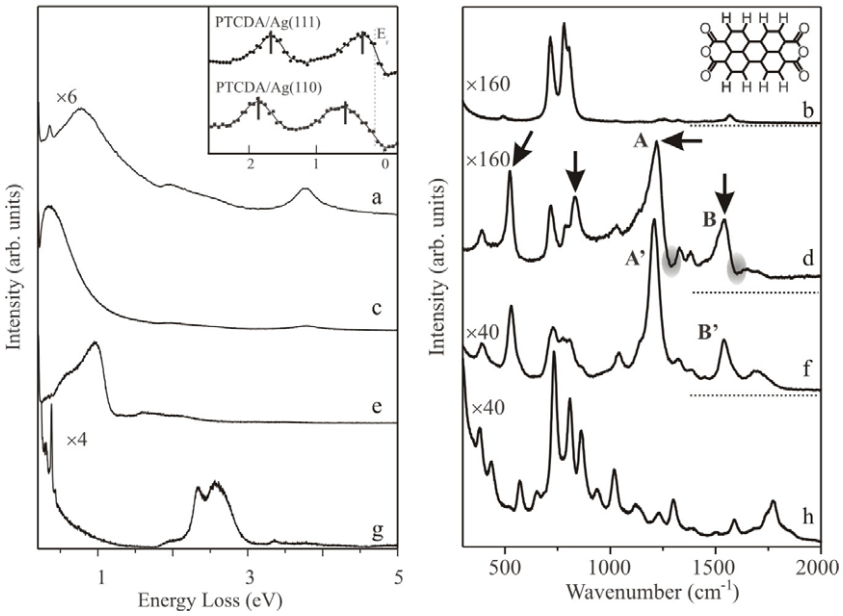

Figure 7. Specular electron energy loss spectra in the energy region of electronic transitions ((a), (c), (e), (g)) and in the energy region of vibrational transitions ((b), (d), (f), (h)): (a), (b) 0.3 ML PTCDA/Ag(110); (c), (d) 0.3 ML PTCDA/Ag(111); (e), (f) 3ML PTCDA/Ag(110) doped with 1.5 K atoms per PTCDA; (g), (h) 20 ML PTCDA on Ag. Inset: UPS spectra of submonolayer PTCDA on Ag(111) (top curve) and Ag(110) (bottom curve). The Fermi level is indicated by the dashed line. Dotted lines in (b), (d), (f) indicate zero intensity for the respective spectra. This reveals the strong EHP continuum present for PTCDA monolayers on Ag(111). For a full discussion, see main text.

pointed out above that this is in good agreement with other spectroscopic results and the *ab initio* calculation of the full interface presented in figure 5, where two concentric rings of charge accumulation are seen, one of which indeed coincides with the central benzene ring of the molecule.

To stress the role of the chemical interaction for mode-selective EHP coupling and IDCT, we finally compare the results on PTCDA/Ag(111) to PTCDA/Au(111). For the latter, the bias dependence in STM images of the first monolayer herringbone structure is very weak [28, 62], indicating the absence of prominent features in the local density of states close to the Fermi level. Also, the surface state of Au(111) is imaged through the PTCDA layer on Au(111) [24, 28]. Finally, high-resolution EELS (HREELS) experiments [22] show an essentially unchanged molecule at the metal interface. Thus this system shows essentially physisorptive bonding. In full accord with the above analysis, a more or less homogeneous broadening of the adsorbate vibrations and no noticeable line shape effects are found for PTCDA on Au(111) [22]. Similarly, the activation via coupling to EHP is essentially absent. We can therefore conclude that the lifetime of all PTCDA vibrations on Au(111) is limited by a non-specific mechanism. At this point, however, a note of caution is in order. The absence of such dramatic dynamic effects as observed for PTCDA on Ag(111) cannot be taken as an indication that the interaction is weak or even not chemisorptive. PTCDA/Ag(110) serves as a counterexample. From structural data it has been argued that the interaction of PTCDA with Ag(110) is at least as strong as for Ag(111) [14]. However, neither a strong continuum of EHP nor IDCT is observed on clean PTCDA/Ag(110) [17]. On the other hand, it is possible to dope PTCDA/Ag(110) by potassium such that, as a function of doping concentration, a semiconductor-to-metal transition is observed, followed by a metal-to-semiconductor transition [63]. In the doped metallic state, IDCT is again observed (cf figures 7(e), (f)).

4. Inelastic tunnelling spectroscopy

Let us now turn to a second experiment in which the coupling between vibrational modes of the adsorbate and its electronic states plays a crucial role. This is the inelastic tunnelling experiment [64]. Here, it is resonantly tunnelling electrons (instead of metal electrons) which, on their passage through the molecule (or more precisely a molecule-derived orbital), interact with molecular vibrations [65]. Although the matrix elements for the damping of vibrations by EHP and the inelastic tunnelling process are the same [12], the processes themselves are quite distinct, such that in general the de-excitation of a molecular vibration by EHP excitation and the excitation of molecular vibrations by tunnelling electrons follow different trends [12]. This difference is also found in the present case.

The inelastic tunnelling process is depicted schematically in figure 8(A) [67]. If the bias voltage exceeds the energy of a vibrational quantum, the tunnelling electron can transfer one vibrational energy quantum to the molecule and still find an empty state in the sample to tunnel into. This opening of a new, inelastic tunnelling channel leads to an abrupt increase in the conductance, or a peak in $\mathrm{d}^2I/\mathrm{d}V^2$ at the vibrational frequency, as shown schematically in figure 8(A). A notable aspect of IETS spectroscopy is the fact that the *excitation* of the vibration is *detected* via its influence on a secondary observable, namely the tunnelling current [12]. Accordingly,

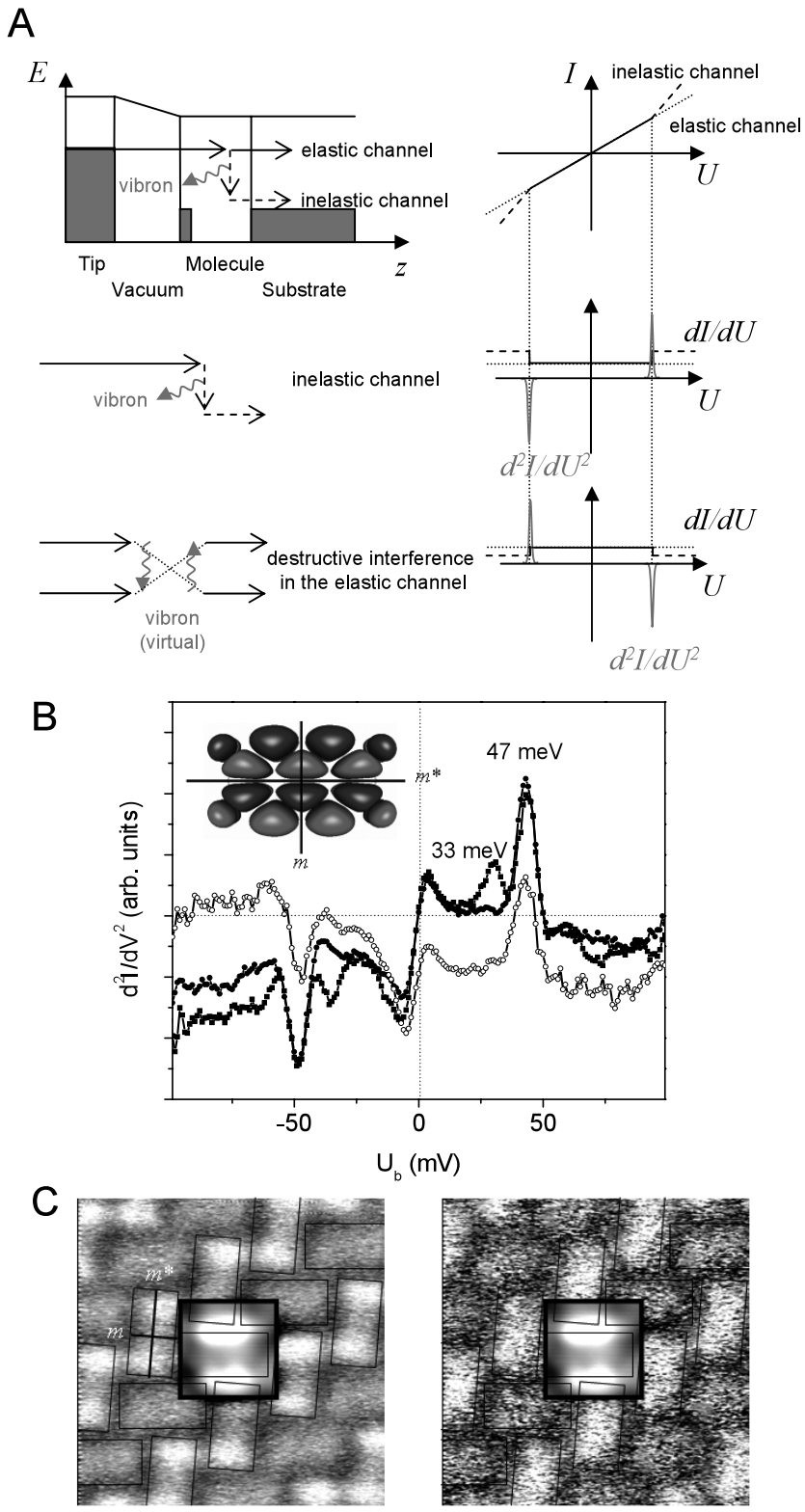

Figure 8. (A) Schematic of the tunnelling process (left) and effect of electron–vibron coupling on the tunnelling current, differential tunnelling conductance $\mathrm{d}I/\mathrm{d}V$ and second derivative $\mathrm{d}^2I/\mathrm{d}V^2$ (right). The coupling of tunnelling electrons to vibrations opens the inelastic channel (top and middle left) and modifies the elastic transport channel (bottom left). Spectral signatures are shown in the corresponding panels on the right. (B) Inelastic tunnelling spectra of PTCDA/Ag(111). Black symbols: molecule of type A (aligned), measured at the maximum intensity of the LUMO (squares) and in the centres of the molecules (circles). Open symbols: molecule of type B (misaligned), measured at point 2. Inset: calculated LUMO orbital of free PTCDA (calculation with Gaussian [72]) with indication of two symmetry planes m and m' and the two points at which measurements have been conducted. (C) Spectroscopic images of the modes at 33 meV (left) and 47 meV (right). The central black frame shows part of the simultaneously recorded topography image, where the molecule is imaged as in figure 1. The thin black line indicates the approximate outline of the molecules.

it is not always true that a large scattering efficiency by a certain vibration will lead to a large step in the current. One possible reason for such a discrepancy is the fact that apart from the *inelastic* scattering of a single electron by a molecular vibration, which opens a new transport channel and leads to a stepwise *in*crease in the conductance, there is a second effect of the molecular vibration on the overall tunnelling current, due to interference between the direct elastic tunnelling path and an elastic path where a virtual vibration is emitted and reabsorbed (cf figure 8(A)) [12, 65, 68]. This *elastic* interference term leads to an abrupt *de*crease in the tunnelling conductance at the threshold energy. Under unfavourable circumstances, the inelastic and elastic vibrational contributions to the tunnelling current may in fact (nearly) cancel each other [12]. Obviously, this possibility presents a complication for the interpretation of spectra.

In fact, it has been found that the interpretation of IETS spectra is often difficult, because (1) only a small fraction of all the vibrational modes of a molecule is usually observed, (2) the scattering cross sections do not follow infrared or Raman selection rules, (3) the inelastic and elastic contributions mentioned above may cancel, and (4) the observed mode activity depends on the adsorption symmetry, geometry and electronic structure [12]. Indeed, the exact nature of excitation–detection selection rules of the IETS process are not (yet) known, making it impossible to predict, on general principles, which modes for a particular molecule can be observed. However, it is clear that STM-based IETS, where electrons are injected very close to the molecules and impact scattering is the dominant interacting mechanism [69], must be distinguished from conventional IETS in oxide junctions, in which the excitation mechanism is the dipole interaction [12]. Usually it is assumed that the vibrational relaxation time is much shorter than the time between successive tunnelling electrons [70] such that only single excitations occur, while the residence time of an individual electron in the molecule is much shorter than any timescale related to the molecule [12].

Complementary to the study of vibrational coupling to EHP, we have studied inelastic tunnelling at the PTCDA/Ag(111) interface systematically. Figure 8(B) displays spectra recorded on both molecules of the herringbone pattern, types A and B, in two different locations, namely in the centre of the molecule and in the maximum of the partially occupied frontier orbital. The results can be summarized as follows. First, in the frequency window from 0 to 200 meV we observe two strong modes, at 33 meV and at 46 meV, respectively. Because the observed peaks correspond to *increasing* conductances, these modes appear in the spectra via inelastic tunnelling, while the elastic effect, if present at all, is at least not dominant. Second, the effect of the modes on the inelastic conductance depends on the position at which the tunnelling current is injected into the molecule. For the mode at $h\nu_1 = 33$ meV, no inelastic conductance contribution occurs if the current is injected into the centre of the molecule, while the mode at $h\nu_2 = 46$ meV shows no such dependence. Third, there is no detectable dependence of the spectra on the type of molecule, except the difference in the strength of the conductance step, which is larger for the aligned molecule (2.0%) than for the misaligned molecule (0.4%).

The latter two observations can be explained on the basis of standard theory of the inelastic tunnelling process. Let us first turn to the strength of the conductance steps. Following the theory of Lorente and Persson [65], one expects the peaks to increase with increasing density of states at the Fermi level. We have seen in figure 2 that due to differences in the molecule–molecule and molecule–substrate interactions, the LUMO of the misaligned molecule is positioned 160 meV below the LUMO of the aligned molecule (figure 2). As a consequence, its density of states at the Fermi level is indeed lower, explaining the smaller inelastic cross section. Typically, conductance steps range between 1% and 10% [12]. The conductance step of 2.0% for molecule A is moderate, while 0.4% for B is rather small.

The dependence of the inelastic current on the injection position can be further investigated by spectroscopic mapping, which is a unique feature of STM-based vibrational spectroscopy. In fact, under certain circumstances, mapping allows mode symmetry determinations, which can be of great help in mode assignments; see, for example, [71]. The matrix element of the scattering process is calculated as the integral over the product between the orbital into which the electron tunnels resonantly (initial state), the vibrational coupling operator (which has the same symmetry as the corresponding vibrational mode), and the final state into which the electron is scattered by the interaction with the vibration [12]. The symmetry of the final state is revealed by the spectroscopic image of the second derivative $\mathrm{d}^2I/\mathrm{d}V^2$, because this image directly shows the transmittance of the molecule for the inelastic current. Recording such a spectroscopic image at the energy of each vibration, we can thus experimentally determine the symmetry of the final state. Since the symmetry of the initial state, i.e. in our case the former LUMO of PTCDA, is also known from spectroscopic imaging of the first derivative $\mathrm{d}I/\mathrm{d}V$ (or even simple imaging, cf figure 1), the symmetry of the two observed vibrations can be determined from experiment, if we assume that the hybridization of the LUMO with the metal states does not change its symmetry.

Considering the adsorbed molecule A first, this adsorbate (including the substrate atoms) has two mutually perpendicular mirror planes: one spanned by the surface normal and the short axis of the molecule (m); the other spanned by the surface normal and the long axis of the molecule (m'). With respect to $m(m')$, the LUMO is even (odd). Turning to the spectroscopic images of the inelastic tunnelling current, we note that scattering from the low-frequency mode ν_1 is not observed in the centre and on the short axis of the molecule. Apparently, the final state of the electron after being scattered inelastically on $h\nu_1$ has a node there, suggesting that it is odd with respect to m. On the other hand, no node of the final state is observed along the long axis, indicating even symmetry of the final state after scattering from $h\nu_1$. We hence must conclude that the low-frequency vibration $h\nu_1$ is odd with respect to both m and m'. A similar analysis for the high-frequency mode $h\nu_2$ shows that it is even with respect to m and odd with respect to m'.

Having determined the symmetry of the two vibrational modes observed in IETS at the PTCDA/Ag(111) interface, the

question regarding the exact nature of these two vibrations arises. Since only two modes are seen at all, although many more exist in the investigated energy range up to 200 meV (the still relatively small number observed in HREELS spectra arises because of surface selection rule in specular scattering, a rule which does not apply to IETS), we may speculate that these two modes form a pair with similar displacement patterns which lead to similarly large cross sections, but with distinct symmetries as specified above. We have used the quantum chemical package Gaussian [72] to conduct DFT calculations with the B3LYP hybrid functional for the isolated PTCDA molecule and determined its vibrational spectrum [22]. A systematic evaluation shows that the only pair of modes with mutually similar displacement patterns *and* the correct symmetries occurs at the calculated energies 32 and 43 meV. Since these calculated frequencies are in excellent agreement with the observed ones, we preliminarily assign the modes in figure 8(B) to these vibrations. At the same time, it is currently not clear why these two modes exhibit a much larger inelastic cross section than all the other 106 modes. In particular, a comparison with monolayer HREELS spectra shows that the propensity rules for dipole scattering at the surface and for inelastic scattering of tunnelling electrons are not the same, although in both spectroscopies those vibrational modes that couple strongly to molecular states at the Fermi level should contribute strongest. But, as already mentioned above, the two spectroscopies probe different types of activities: for a strong IDCT signal in HREELS, a strong modulation of the energetic position of the partially occupied molecular orbital close to the Fermi level is required, while for STM-IETS a strong modulation of the wavefunction tails, belonging to states at the Fermi level, at the position of the tip apex is beneficial [12].

5. Conclusion

In this article, the influence of the chemical interaction between a large π-conjugated molecule and a noble-metal surface on the electron–vibron coupling at the interface has been discussed. Both the interfacial dynamical charge transfer detected in electron energy loss spectroscopy and the results of inelastic tunnelling spectroscopy are in qualitative agreement with the picture of the chemical bond that was derived from a direct investigation of the electronic structure. However, it must be stressed that the calculations of the dynamical properties which we have used for rationalizing the data of both experiments have been performed on the free molecule. Since it is well known that the vibrational properties of the adsorbate may be modified by the interaction with the substrate, full simulations of the dynamical properties of the interface, and in particular of electron–vibron coupling effects such as IDCT and IETS, are still necessary. As geometrical and electronic structure calculations of the PTCDA/Ag(111) interface are already available, the dynamic properties, as revealed in IETS and dipole HREELS, could turn out to be a sensitive benchmark to validate the theoretical description in these calculations. This is important, because weakly interacting interfaces such as our example are a challenge to DFT, and properties which depend sensitively on the predicted electronic structure should therefore be particularly valuable for a validation of the electronic structure calculations. Theoretical calculations of the dynamic properties of the full PTCDA/Ag(111) interface are currently in progress.

The first realization of STM-based IETS in 1998 by Ho *et al* [64] was generally considered to be a breakthrough in the long-running attempts to make STM chemically sensitive. After all, vibrational spectroscopy is used routinely in chemistry to identify molecules by their vibrational fingerprints, and inelastic tunnelling spectroscopy in metal–oxide–metal junctions had been known as a powerful vibrational spectroscopy since the 1960s. However, the initial euphoria concerning STM-based IETS as a spectroscopic tool has been dampened by the fact that, on all but the smallest molecules, STM-based IETS does not seem to provide vibrational fingerprints of sufficient detail to identify a single adsorbate molecule by comparison with a database of known vibrational spectra. The present results on PTCDA/Ag(111) once more confirm this general finding.

Quite apart from the potential to identify unknown molecular species, IETS as a single-molecule spectroscopy could offer the capability to assign certain spectral features to individual molecules in an inhomogeneous ensemble, and thus use molecular vibrations as specific probes of the molecule–molecule and molecule–substrate interactions. The adsorption system PTCDA/Ag(111) is a valuable test-bed in this context, because the monolayer contains two different molecules in distinct adsorption configurations with slightly different chemical substrate interactions and intermolecular interactions. However, in our IETS experiments on this interface it has turned out to be impossible to resolve differences in the vibrational frequencies between molecules of types A and B. Apparently, the small number of observable modes and their relatively weak cross sections are too strong a limitation for such an analysis in the present case. However, it also may be true that the differences in the intermolecular and molecule–substrate interactions (which are observed in the differential conductance STS spectra) only have a minor effect on the molecular vibrations, beyond the resolution of the present IETS experiment. Again, only a first-principles theoretical analysis of the dynamical properties of this adsorbate system will be able to tell.

References

[1] Shinar J (ed) 2004 *Organic Light-Emitting Devices: A Survey* (New York: Springer)
[2] Yersin H (ed) 2007 *Highly Efficient OLEDs with Phosphorescent Materials* (New York: Wiley–VCH)
[3] Facchetti A 2007 *Mater. Today* **10** 28
[4] Klauk H (ed) 2006 *Organic Electronics: Materials, Manufacturing, and Applications* (Weinheim: Wiley–VCH)
[5] Hoppe H and Sariciftci N S 2004 *J. Mater. Res.* **19** 1924
[6] Soubatch S, Temirov R and Tautz F S 2008 *Phys. Stat. Sol. A* **205** doi:10.1002/pssa.200723447
[7] Zou Y, Kilian L, Scholl A, Schmidt T, Fink R and Umbach E 2006 *Surf. Sci.* **600** 1240
[8] Rohlfing M, Temirov R and Tautz F S 2007 *Phys. Rev.* B **76** 115421
[9] Kröger J 2006 *Rep. Prog. Phys.* **69** 899
[10] Tautz F S 2007 *Prog. Surf. Sci.* **82** 479

[11] Tautz F S, Eremtchenko M, Schaefer J A, Sokolowski M, Shklover V and Umbach E 2002 *Phys. Rev.* B **65** 125405
[12] Pascual J I and Lorente N 2006 *Single-Molecule Vibrational Spectroscopy and Chemistry* ed P Grütter, W Hofer and F Rosei (Singapore: World Scientific)
[13] Eremtchenko M, Schaefer J A and Tautz F S 2003 *Nature* **425** 602
[14] Glöckler K, Seidel C, Soukopp A, Sokolowski M, Umbach E, Böhringer M, Berndt R and Schneider W D 1998 *Surf. Sci.* **405** 1
[15] Hauschild A, Karki K, Cowie B C C, Rohlfing M, Tautz F S and Sokolowski M 2005 *Phys. Rev. Lett.* **95** 209602
[16] Hauschild A, Karki K, Cowie B C C, Rohlfing M, Tautz F S and Sokolowski M 2005 *Phys. Rev. Lett.* **94** 036106
[17] Shklover V, Tautz F S, Scholz R, Sloboshanin S, Sokolowski M, Schaefer J A and Umbach E 2000 *Surf. Sci.* **454** 60
[18] Sokolowski M, Schneider M and Umbach E 2006 *Chem. Phys.* **325** 185
[19] Temirov R, Soubatch S, Luican A and Tautz F S 2006 *Nature* **444** 350
[20] Umbach E, Glöckler K and Sokolowski M 1998 *Surf. Sci.* **404** 20
[21] Kraft A, Temirov R, Henze S K M, Soubatch S, Rohlfing M and Tautz F S 2006 *Phys. Rev.* B **74** 041402(R)
[22] Eremtchenko M, Bauer D, Schaefer J A and Tautz F S 2004 *New J. Phys.* **6** 4
[23] Schmitz-Hübsch T, Fritz T, Sellam F, Staub R and Leo K 1997 *Phys. Rev.* B **55** 7972
[24] Chizhov I, Kahn A and Scoles G 2000 *J. Cryst. Growth* **208** 449
[25] Kilian L 2002 *PhD Thesis* University of Würzburg
[26] Weinhold M, Soubatch S and Tautz F S, unpublished
[27] Henze S K M, Bauer O, Lee T L, Sokolowski M and Tautz F S 2007 *Surf. Sci.* **601** 1566
[28] Nicoara N, Roman E, Gomez-Rodriguez J M, Martin-Gago J A and Mendez J 2006 *Org. Electron.* **7** 287
[29] Tautz F S, unpublished
[30] Du S X, Gao H J, Seidel C, Tsetseris L, Ji W, Kopf H, Chi L F, Fuchs H, Pennycook S J and Pantelides S T 2006 *Phys. Rev. Lett.* **97** 156105
[31] Ji W, Lu Z-Y and Gao H 2006 *Phys. Rev. Lett.* **97** 246101
[32] Picozzi S, Pecchia A, Gheorghe M, Di Carlo A, Lugli P, Delley B and Elstner M 2003 *Phys. Rev.* B **68** 195309
[33] Rurali R, Lorente N and Ordejon P 2005 *Phys. Rev. Lett.* **95** 209601
[34] Eremtchenko M, Bauer D, Schaefer J A and Tautz F S 2004 *J. Mater. Res.* **19** 2028
[35] Head-Gordon M and Tully J C 1995 *J. Chem. Phys.* **103** 10137
[36] Kindt J T, Tully J C, Head-Gordon M and Gomez M A 1998 *J. Chem. Phys.* **109** 3629
[37] Tully J C, Gomez M and Headgordon M 1993 *J. Vac. Sci. Technol.* A **11** 1914
[38] Tully J C 2000 *Annu. Rev. Phys. Chem.* **51** 153
[39] Chance R R, Prock A and Silbey R 1975 *J. Chem. Phys.* **62** 2245
[40] Persson B N J 1978 *J. Phys. C: Solid State Phys.* **11** 4251
[41] Hirschmugl C J 2002 *Surf. Sci.* **500** 577
[42] Langreth D C and Persson M 1995 *Vibrational Relaxation and Dephasing of Molecules Adsorbed on Metal Surfaces* ed H L Dai and W Ho (Singapore: World Scientific)
[43] Persson B N J and Persson M 1980 *Solid State Commun.* **36** 175
[44] Persson B N J 1987 *Chem. Phys. Lett.* **139** 457
[45] Persson B N J and Ryberg R 1982 *Phys. Rev. Lett.* **48** 549
[46] Hirschmugl C J, Chabal Y J, Hoffmann F M and Williams G P 1994 *J. Vac. Sci. Technol.* A **12** 2229
[47] Hirschmugl C J, Williams G P, Hoffmann F M and Chabal Y J 1990 *Phys. Rev. Lett.* **65** 480
[48] Hirschmugl C J, Williams G P, Hoffmann F M and Chabal Y J 1990 *J. Electron Spectrosc. Relat. Phenom.* **54/55** 109
[49] Hirschmugl C J, Williams G P, Persson B N J and Volokitin A I 1994 *Surf. Sci.* **317** L1141
[50] Peremans A, Caudano Y, Thiry P A, Dumas P, Zhang W Q, LeRille A and Tadjeddine A 1997 *Phys. Rev. Lett.* **78** 2999
[51] Rudolf P, Raval R, Dumas P and Williams G P 2002 *Appl. Phys.* A **75** 147
[52] Silien C, Caudano Y, Longueville J L, Bouzidi S, Wiame F, Peremans A and Thiry P A 1999 *Surf. Sci.* **427/428** 79
[53] Silien C, Caudano Y, Peremans A and Thiry P A 2000 *Appl. Surf. Sci.* **162** 445
[54] Tautz F S, Eremtchenko M, Schaefer J A, Sokolowski M, Shklover V, Glöckler K and Umbach E 2002 *Surf. Sci.* **502** 176
[55] Fano U 1961 *Phys. Rev.* **124** 1866
[56] Crljen Z and Langreth D C 1987 *Phys. Rev.* B **35** 4224
[57] Langreth D C 1985 *Phys. Rev. Lett.* **54** 126
[58] Rice M J 1979 *Solid State Commun.* **31** 93
[59] Rice M J, Lipari N O and Strassler S 1977 *Phys. Rev. Lett.* **39** 1359
[60] Rice M J, Yartsev V M and Jacobsen C S 1980 *Phys. Rev.* B **21** 3437
[61] Devos A and Lannoo M 1998 *Phys. Rev.* B **58** 8236
[62] Kröger J, Jensen H, Berndt R, Rurali R and Lorente N 2007 *Chem. Phys. Lett.* **438** 249
[63] Shklover V, Schmitt S, Umbach E, Tautz F S, Eremtchenko M, Shostak Y, Schaefer J A and Sokolowski M 2001 *Surf. Sci.* **482** 1241
[64] Stipe B C, Rezaei M A and Ho W 1998 *Science* **280** 1732
[65] Lorente N and Persson M 2000 *Phys. Rev. Lett.* **85** 2997
[66] Lorente N and Persson M 2000 *Faraday Discuss.* **117** 277
[67] Pascual J I and Lorente N 2006 Inelastic electron tunneling microscopy and spectroscopy of single molecules by STM *Scanning Probe Microscopies Beyond Imaging* ed P Samori (Winheim: Wiley–VCH)
[68] Lorente N 2004 *Appl. Phys.* A **78** 799
[69] Persson B N J and Baratoff A 1987 *Phys. Rev. Lett.* **59** 339
[70] Persson M 2004 *Phil. Trans. R. Soc.* A **362** 1173
[71] Bocquet M L, Lesnard H and Lorente N 2006 *Phys. Rev. Lett.* **96** 096101
[72] Frisch M J *et al* 2004 *Gaussian 03.* Gaussian Inc.